

Hierarchical Multi-Agent DRL Based Dynamic Cluster Reconfiguration for UAV Mobility Management

Irshad A. Meer, *Student Member, IEEE*, Karl-Ludwig Besser, *Member, IEEE*, Mustafa Ozger, *Member, IEEE*, Dominic Schupke, *Member, IEEE*, H. Vincent Poor, *Life Fellow, IEEE*, and Cicek Cavdar, *Member, IEEE*

Abstract—Multi-connectivity involves dynamic cluster formation among distributed access points (APs) and coordinated resource allocation from these APs, highlighting the need for efficient mobility management strategies for users with multi-connectivity. In this paper, we propose a novel mobility management scheme for unmanned aerial vehicles (UAVs) that uses dynamic cluster reconfiguration with energy-efficient power allocation in a wireless interference network. Our objective encompasses meeting stringent reliability demands, minimizing joint power consumption, and reducing the frequency of cluster reconfiguration. To achieve these objectives, we propose a hierarchical multi-agent deep reinforcement learning (H-MADRL) framework, specifically tailored for dynamic clustering and power allocation. The edge cloud connected with a set of APs through low latency optical back-haul links hosts the high-level agent responsible for the optimal clustering policy, while low-level agents reside in the APs and are responsible for the power allocation policy. To further improve the learning efficiency, we propose a novel action-observation transition-driven learning algorithm that allows the low-level agents to use the action space from the high-level agent as part of the local observation space. This allows the lower-level agents to share partial information about the clustering policy and allocate the power more efficiently. The simulation results demonstrate that our proposed distributed algorithm achieves comparable performance to the centralized algorithm. Additionally, it offers better scalability, as the decision time for clustering and power allocation increases by only 10% when doubling the number of APs, compared to a 90% increase observed with the centralized approach.

Index Terms—Reinforcement learning, Energy-efficiency maximization, Ultra-reliable communications, UAV communications.

I. INTRODUCTION

In cell-less wireless network, users are no longer connected to just one access point (AP) but are instead served

Parts of this work were presented at the 2024 IEEE International Conference on Machine Learning for Communication and Networking (ICMLCN) [1].

I. A. Meer, M. Ozger, and C. Cavdar are with the School of Electrical Engineering and Computer Science, KTH Royal Institute of Technology, Stockholm, Sweden (e-mail: {iameer, ozger, cavdar}@kth.se). K.-L. Besser, and H. V. Poor are with the Department of Electrical and Computer Engineering, Princeton University, USA (e-mail: {karl.besser, poor}@princeton.edu). D. Schupke is with Airbus, Central Research and Technology, Taufkirchen, 82024 Germany (e-mail: dominic.schupke@airbus.com). M. Ozger is also with the Department of Electronic Systems, Aalborg University, Copenhagen, 2450 Denmark (e-mail: mozger@es.aau.dk).

This work was supported in part by the CELTIC-NEXT Project, 6G for Connected Sky (6G-SKY), with funding received from Vinnova, Swedish Innovation Agency. The work of K.-L. Besser is supported by the German Research Foundation (DFG) under grant BE 8098/1-1. The work of H. V. Poor is supported by the U.S. National Science Foundation under Grants CNS-2128448 and ECCS-2335876.

simultaneously in non-orthogonal multiple access schemes by numerous distributed APs [2]. This shift dramatically alters the traditional approach to mobility management, moving away from standard handover management to a more dynamic cluster reconfiguration model [1], [3]. As a result, the traditional concept of coverage is transformed from being cell-centric to being user-centric.

In this model, users are now seamlessly supported by a group of multiple distributed APs using the same frequency-time resources. The cooperation of APs to form clusters and serve users can be implemented using various techniques, such as coordinated multi-point (CoMP) [4], cloud-radio access network (C-RAN) [5], and cell-free networks [6]. However, determining the optimal cluster of the APs, i.e., the cluster configuration, to satisfy stringent quality of service (QoS) requirements, such as reliability, in dynamic environments, where the user's location continuously changes is a major challenge. Moreover, the cluster configuration must simultaneously meet multiple, often conflicting objectives. While providing communication through multiple APs can enhance QoS, it may also result in excessive power consumption due to the simultaneous transmission from different APs within the cluster. Thus, a critical factor is minimizing total transmission power while maintaining the high reliability demands by modern applications. The high mobility of unmanned aerial vehicles (UAVs) can also cause frequent cluster reconfigurations, which correspond to the change in the cluster set as well as power levels of the associated APs. Hence, it may lead to increased control overhead and latency to reconfigure the clusters due to the mobility of UAVs.

In addition, developing an efficient power allocation scheme for dynamic clusters in a multi-connectivity wireless interference network presents a significant challenge. This requires continuously adapting to changing network conditions and cluster configurations while managing interference, all under stringent QoS constraints [7]. Different approaches, including optimization theory [8], matching theory [9], [10], and game theory [11] have been explored to address the challenges of dynamic clustering and resource allocation in different networks. However, these conventional techniques are often hindered by several issues. For example, they depend on having complete and real-time information about network dynamics, which is unrealistic in a wireless scenario where channel conditions fluctuate rapidly, especially for UAV communication having a probabilistic line of sight conditions with ground APs.

Additionally, These methods are computationally intensive and struggle to scale, with complexity increasing exponentially as network size grows [2].

Machine learning (ML), especially deep reinforcement learning (DRL), has been recognized as a more adaptable and resilient method for managing cluster reconfiguration and resource allocation, by interacting with an unpredictable wireless environment [1], [3], [12], [13]. Through environmental learning, DRL leverages unique characteristics of communication networks to learn the desired policies. While a centralized DRL approach can efficiently solve the cluster reconfiguration and resource allocation problem [1], it faces scalability issues as the network size increases. On the other hand, multi-agent deep reinforcement learning (MADRL) addresses scalability by enabling distributed decision-making. However, despite its scalability advantages, MADRL encounters performance limitations due to the lack of global information, which can affect coordination and overall efficiency [14]. As a result, both approaches present distinct advantages and challenges that must be balanced. This motivates the use of hierarchical MADRL, which combines local decision-making with a higher-level coordination structure, offering a potential solution to both scalability and performance trade-offs.

In this paper, we provide a scalable mobility management framework for the multi-connectivity scenario, which meets stringent reliability requirements while minimizing transmit power and the number of cluster reconfigurations, even when the network size increases. Given the uncertainties in UAVs mobility and the variability of channel conditions over time, we model the joint problem of cluster reconfiguration and power allocation as a Markov decision process (MDP) and propose a hierarchical MADRL framework to solve it. A high-level agent operates within the edge cloud and makes the clustering decision, while multiple low-level agents each associated with individual AP perform power allocation to the assigned users, as shown in Figure 1. The core concept involves decentralizing the decision-making process, assigning responsibilities to different levels of the network rather than relying on a single decision-making agent. To improve the performance of hierarchical MADRL and provide the low level agents with global environmental information for better decision making, we propose a novel action-observation transition mechanism. This mechanism allows the action from the higher agent to be used as a part of the observation space of the low level agents.

The main contributions are summarized below.

- We formulate an optimization problem focused on dynamic clustering of APs and their power allocation for UAVs within a wireless interference network. The objective is to satisfy the stringent reliability requirements, specifically considering error probabilities in finite block-length regimes, reduce power consumption, and minimize the frequency of cluster reconfigurations.
- We propose a hierarchical MADRL approach to enhance communication reliability, lower power consumption, and minimize cluster reconfiguration frequency in a dynamic environment while improving the scalability and reducing complexity and overhead. The high-level agent in the edge

cloud, connected to the APs, optimizes the AP clustering strategy, while the low-level AP agents optimize the power allocation. Additionally, the APs' power allocation strategies influence the edge cloud's clustering strategy, further improving system performance.

- We further propose an action-observation transition-driven hierarchical framework, where the observation space of the low-level agents includes the actions of the higher-level agent. This integration ensures that the decisions made by the higher-level agent directly influence and guide the behavior of the low-level agents, creating a more cohesive and adaptive system for multi-connectivity mobility management.
- Finally, we validate the feasibility of our proposed hierarchical MADRL through numerical simulations. The results show that our proposed algorithm can achieve better performance in comparison with other existing works, including the central clustering approach in [1] and the opportunistic clustering algorithm in [15].

II. RELATED WORK

Recently, mobility management for aerial users in mobile networks has emerged as a key research focus. In conventional single-connectivity mobile networks, several studies [16]–[20] have approached the handover problem by modeling it as an optimization task and leveraging DRL algorithms to make handover decisions. For example, [16] compares model-based and deep Q-network (DQN)-based strategies for managing handovers in single-connectivity cellular-connected UAVs. Similarly, [17] implements a DQN-based policy to optimize handover rates and user throughput. The authors in [18] use Q-learning to reduce the number of handovers and enhance signal quality by introducing an reinforcement learning (RL)-based framework that balances handovers and received signal strength for connected UAVs. In [19], an RL-based handover management scheme is proposed to jointly optimize communication delay, interference, and handover frequency, focusing on reducing uplink interference from UAVs. Lastly, [20] jointly optimizes handover decisions, interference, communication delay, and UAV path using a DRL-based framework.

While the aforementioned studies address mobility management for single-connectivity aerial users, mobility management for aerial users served via multi-connectivity in mobile networks is considerably more complex. In multi-connectivity scenarios, each user has multiple candidate APs forming a cluster to serve. However, this leads to an exponentially larger action space, which makes convergence difficult. In [15], a dynamic clustering approach is employed in an open-radio access network (O-RAN) architecture based on channel gains between the user and the APs. Although this method does not involve learning, it increases signal overhead and requires cluster reconfiguration whenever a user is added or removed. In [21], beamforming vectors for dynamic AP clustering are designed using RL for terrestrial users. However, the proposed method does not address aerial users with stringent reliability requirements. The work in [22] focuses on varying reliability

Table I
TABLE OF NOTATION

Notation	Definition
\mathcal{K}, k, K	The set, the index and the number of APs
\mathcal{N}, i, N	The set, the index and the number of AUs
$h_{ik}(t)$	Channel gain from AP k to AU i at time t
Γ	Clustering strategy at the edge cloud
\mathcal{N}_k	Set of assigned users to AP k , $\mathcal{N}_k \subseteq \mathcal{N}$
\mathcal{M}_i	Serving cluster for AU i
$P_{T,ik}(t)$	Transmitted power from AP k to AU i
$P_i(t)$	Received power at user i
P_{max}	Maximum allowed transmit power
N_0	Noise spectral density
G_0	Antenna array gain
$\theta_{i,k}(t)$	Elevation angle between AP k and AU i
$\phi_{i,k}(t)$	Azimuth angle between AP k and AU i
$\gamma_i^{\mathcal{M}_i}$	Receive SINR at AU i served by cluster \mathcal{M}_i
b_i	Number of transmitted information bits to user i
n	Finite block-length
ε_i	Decoding error probability at AU i
ε_{max}	Maximum acceptable error probability
γ^{th}	SINR threshold
$O_i(t)$	SINR outage probability of AU i

for aerial users served by cluster of terrestrial APs but limits its analysis to non-interfering environments with a single user. Matching theory has also been applied to achieve optimal clustering in multi-connectivity mobility scenarios [9], [10]; however, this approach is based on a static snapshot model, which does not account for the dynamic challenges inherent in the problem.

Hierarchical deep reinforcement learning (HDRL) has emerged as a promising solution for addressing complex optimization problems by breaking them down into smaller, more manageable subproblems [23], [24]. In [23], HDRL was applied to a drone cell trajectory planning and resource allocation problem by decomposing it into two subproblems: higher-level global trajectory planning and lower-level local resource allocation. Likewise, [24] tackled the joint problem of radio access technologies (RATs) assignment and power allocation by leveraging the HDRL framework to divide the problem into two stages: RATs-user assignment and power allocation. More recently, [25] extended HDRL to handle handover management and power allocation for terrestrial users. However, they do not consider stringent reliability requirements in the finite block-length regime.

To the best of our knowledge, there is limited research focusing on energy-efficient mobility management solutions that meet stringent reliability requirements in the finite block-length regime for aerial users with multi-connectivity configuration in mobile networks.

III. SYSTEM MODEL AND PROBLEM FORMULATION

We consider an O-RAN architecture with a downlink communication scenario, where the communication is established from a cluster of APs to the UAVs. In a given area, we have K O-RAN radio units (O-RUs) (hereafter referred to as APs)

deployed at fixed locations. All the APs are connected to the edge cloud with virtualization and processing resource-sharing capabilities [26]. A total of N UAVs, also referred to as AUs, are moving within the coverage area following a 3D stochastic mobility model from [27]. All the AUs are equipped with a single omnidirectional antenna while each APs is equipped with L uniform planar array antennas. The notation used in the paper are given in the Table I. When AU i enters the coverage area of the edge cloud, a cluster of APs under the clustering strategy Γ form the cluster to serve AU i . A general clustering strategy is defined as follows.

Definition 1. A clustering strategy Γ defines a collection $\{\mathcal{M}_1^\Gamma, \mathcal{M}_2^\Gamma, \dots, \mathcal{M}_N^\Gamma\}$ of subsets of \mathcal{K} , where $\mathcal{M}_i^\Gamma \subseteq \mathcal{K}$ is referred to as the serving cluster for AU i , with $|\mathcal{M}_i^\Gamma| \geq 1$ and $|\bigcup_{i=1}^N \mathcal{M}_i^\Gamma| \leq K$.

Note that the clusters \mathcal{M}_i^Γ may overlap, and their union may not necessarily cover all elements of \mathcal{K} . Therefore, the total received power P_i at AU i at time t is given as

$$P_i(t) = \sum_{k=1}^{|\mathcal{M}_i^\Gamma(t)|} h_{ik}(t) P_{T,ik}(t) G(\theta_{i,k}(t), \phi_{i,k}(t)), \quad (1)$$

where $P_{T,ik}$ denotes the transmit power of AP k to user i , and h_{ik} is the power attenuation between APs k and user i , i.e., the combined path loss and fading effects. These effects are modeled according to [28]. With known location of the user, we incorporate the 3D beamforming and beamtracking by leveraging the antenna radiation pattern and the steering vectors [29]. For this, $G(\theta_{i,k}(t), \phi_{i,k}(t))$ represents the antenna array gain from AP k to user i , which is located at an elevation angle of $\theta_{i,k}(t)$ and azimuth angle of $\phi_{i,k}(t)$ with respect to the APs. The antenna array gain is given by

$$G(\theta_{i,k}(t), \phi_{i,k}(t)) = G_0 \cdot \mathbf{a}(\theta_{i,k}(t)) \cdot \mathbf{b}(\phi_{i,k}(t)),$$

where G_0 represents the constant array gain, while $\mathbf{a}(\theta_{i,k}(t))$ and $\mathbf{b}(\phi_{i,k}(t))$ represent the steering vectors in the elevation and azimuth directions, respectively. The vectors $\mathbf{a}(\theta_{i,k}(t))$ and $\mathbf{b}(\phi_{i,k}(t))$ are given according to [29] as

$$\mathbf{a}(\theta_i) = \sum_{m=1}^M \mathbf{I}_m e^{j(m-1)(kd_z \cos(\theta_i))}, \quad (2)$$

$$\mathbf{b}(\phi_i) = \sum_{n=1}^N \mathbf{I}_n^T e^{j(n-1)(kd_y \sin(\theta_i) \sin(\phi_i))}, \quad (3)$$

where, \mathbf{I}_m and \mathbf{I}_n denote column vectors of ones of sizes m and n , respectively. The number of antennas in z - and y -directions of the antenna array are M and N , respectively. The d_z and d_y represent the antenna spacing in the z - and y -directions, respectively, and k represents the wave number. For ease of reading, we omit the time index t and the superscript Γ , unless it is necessary to explicitly specify it.

Definition 2. For a given clustering strategy Γ , a power allocation policy $P_{T,ik}$ defines power allocation in each cluster i , $\{P_{T,i1}, P_{T,i2}, \dots, P_{T,iK}\}$, where $P_{T,ik}$ is the allocated power from AP k to AU i .

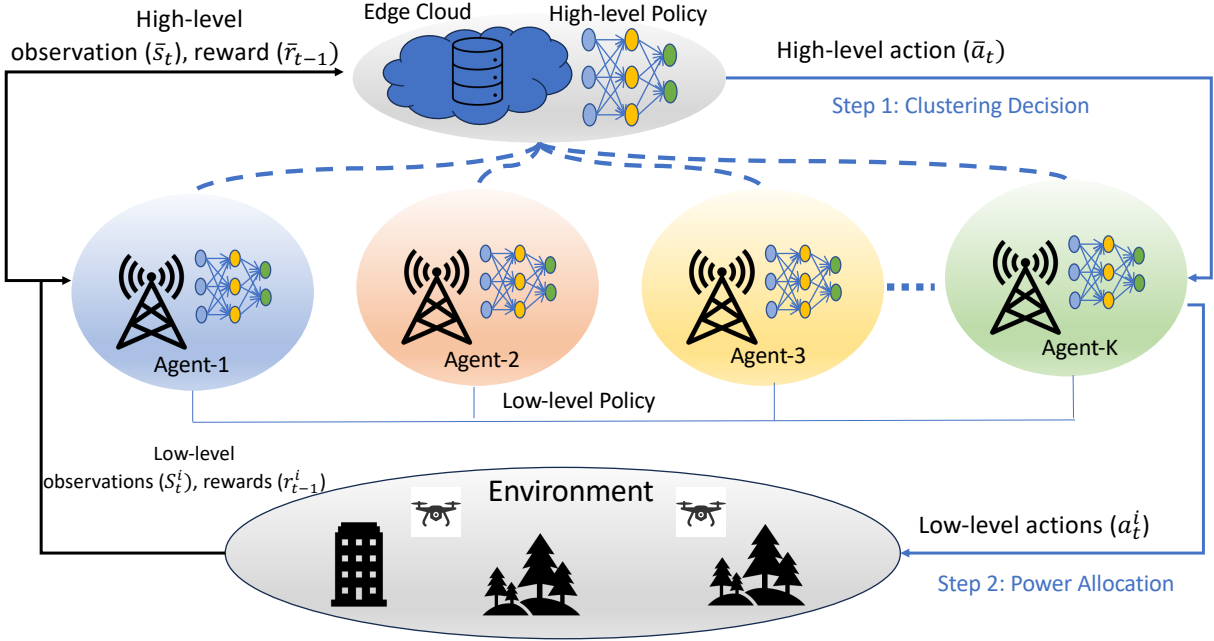


Figure 1. Network architecture of the proposed H-MAPPO. The system consists of K multi-agents at the APs, connected to a high-level agent in the edge cloud. These agents collaboratively serve N AUs. The H-MAPPO framework operates in two steps: (1) the high-level agent makes a clustering decision and communicates it to the low-level agents; (2) the low-level agents allocate power to the assigned AUs based on the clustering information and local observations.

With the above definition, the receive signal-to-interference-plus-noise ratio (SINR) at the target AU i served by cluster \mathcal{M}_i is:

$$\gamma_i^{\mathcal{M}_i} = \frac{\sum_{k=1}^{|\mathcal{M}_i|} h_{ik} P_{T,ik} G(\theta_{i,k}, \phi_{i,k})}{\sigma^2 + \sum_{k=1}^K \sum_{\substack{n=1 \\ n \neq i}}^N h_{kn} P_{T,nk} G(\theta_{n,k}, \phi_{n,k})}, \quad (4)$$

where σ^2 is the noise power, and the interference power is the sum of all received power from all APs serving on the same resource to other AUs.

A. Finite Block-length Case

UAV applications such as real-time surveillance, emergency response, and industrial inspection require not only seamless service continuity for payload traffic but also ultra-reliable low latency communication (URLLC) for command and control operations. Such communication relies on finite block-length codes, where the decoding error probability is non-zero, thus affecting the reliability. Multi-connectivity has been shown to improve URLLC in such finite block-length regimes [30]–[32]. Therefore, our goal is to investigate the impact of cluster reconfiguration and power allocation in this finite block-length regime.

Assuming white Gaussian noise, the channel capacity as a function of the SINR at the AU i is given by:

$$C(\gamma_i^{\mathcal{M}_i}) = \log_2(1 + \gamma_i^{\mathcal{M}_i}). \quad (5)$$

In the finite block-length regime, there is an approximation for the maximum achievable rate, accounting for the finite sample size, error probability, and coding. The data rate for

AU i with block-length n and error probability ε is given by [33, Eq. (296)]:

$$R_i^*(n, \varepsilon) \approx \mathbb{E} \left\{ C(\gamma_i^{\mathcal{M}_i}) - \sqrt{\frac{V(\gamma_i^{\mathcal{M}_i})}{n}} Q^{-1}(\varepsilon_i) + \frac{\log_2 n}{2n} + \mathcal{O}(1) \right\} \quad (6)$$

where Q^{-1} is the inverse Q-function, which is defined as

$$Q(x) = \frac{1}{\sqrt{2\pi}} \int_x^\infty \exp\left(-\frac{t^2}{2}\right) dt.$$

The channel dispersion $V(\gamma_i^{\mathcal{M}_i})$ in (6) is given by

$$V(\gamma_i^{\mathcal{M}_i}) = \left(1 - \frac{1}{(1 + \gamma_i^{\mathcal{M}_i})^2}\right) (\log_2 e)^2. \quad (7)$$

According to (6), using a finite block length results in a maximum achievable rate that is less than the channel capacity (with an infinite block length). This reduction is caused by the channel dispersion $V(\gamma)$. However, as the block length n becomes very large and the error probability ε_i approaches zero, the achievable rate can reach the channel capacity.

The minimum decoding error probability (DEP) incurred in the transmission of b_i bits to AU i using a finite block-length of n can be accurately approximated by substituting $R_i = \frac{b_i}{n}$ in (6) and is given by [34]

$$\varepsilon_i(n, b_i) \approx \mathbb{E} \left\{ Q \left(\frac{nC(\gamma_i^{\mathcal{M}_i}) + \frac{1}{2} \log_2 n - b_i}{\sqrt{nV(\gamma_i^{\mathcal{M}_i})}} \right) \right\}. \quad (8)$$

The expectation in (8) is over $\gamma_i^{\mathcal{M}_i}$ since the SINR changes with different channel realizations. In order to have reliable

communications, the error probability should be less than a maximum threshold, i.e., $\varepsilon_i(n, b_i) \leq \varepsilon_{\max}$. The maximum DEP constraint can also be written as a SINR constraint as

$$\gamma_i^{\mathcal{M}_i} \geq \gamma_{\text{th}} \approx \exp\left(\frac{Q^{-1}(\varepsilon_{\max})}{\sqrt{n}} + \frac{b_i \ln 2}{n} - \frac{\ln n}{2n}\right) - 1. \quad (9)$$

While we assume that the positions of the AUs and the fading statistics are known, the exact channel state is assumed to be unknown. Hence, the user will be in an outage with a non-zero probability when the SINR at the AU is below a predefined threshold γ_{th} , i.e., the outage probability for user i at time t is given as

$$O_i(t) = \Pr\left(\gamma_i^{\mathcal{M}_i}(t) < \gamma_{\text{th}}\right). \quad (10)$$

Depending on the specific use case, there exists an outage probability requirement, denoted as O_{\max} , that is deemed acceptable. However, it is essential to acknowledge that this tolerance level is influenced by various factors and may change over time, e.g., when the user moves into a different area.

B. SINR Outage

In the sequel, we derive an expression for calculating the outage probability from (10) for a single time slot t , i.e., for a fixed power allocation and fixed positions of all users. In this case, we can rewrite the outage probability as the probability of a new random variable that comprises of a sum of exponentially distributed random variables with different expected values,

$$\begin{aligned} O_i(t) &= \Pr\left(\gamma_i^{\mathcal{M}_i}(t) < \gamma_{\text{th}}\right) \\ &= \Pr\left(\sum_{k=1}^{|\mathcal{M}_i|} h_{ik} P_{T,ik} G(\theta_{i,k}, \phi_{i,k}) < s_i\right) \\ &= \Pr\left(\sum_{k=1}^{|\mathcal{M}_i|} Y_{ik} < s_i\right) \\ &= \Pr(T_i < s_i) \\ &= 1 - \bar{F}_{T_i}(s_i) \end{aligned} \quad (11)$$

where $s_i = \gamma_{\text{th}} \beta_i$ is the product of the SINR threshold γ_{th} and the interference power β_i at user i . Based on the Rayleigh fading model, the random variable T_i is given as the sum of exponentially distributed variables $Y_{ik} \sim \text{Exp}(\alpha_{ik})$ with different expected values α_{ik} . The expected values are given by the product of transmit power, antenna gain, and path loss. The survival function \bar{F}_{T_i} of T_i is given by [35]

$$\bar{F}_{T_i}(s) = \sum_{k=1}^K A_{ik} \cdot \exp(-\alpha_{ik} \cdot s), \quad (12)$$

$$A_{ik} = \prod_{\substack{j=1 \\ j \neq k}}^K \frac{\alpha_{ik}}{\alpha_{ij} + \alpha_{ik}}, \quad \text{for } k = 1, \dots, K. \quad (13)$$

For this expression to hold, we need to assume that all α_{ik} are distinct. However, since they are the product of transmit power, antenna gain, and path loss, this assumption will hold almost surely in practice.

C. Problem Formulation

The joint dynamic clustering and power allocation for APs is of utmost importance to ensure both reliable and energy-efficient communication. To accomplish this objective, we present an optimization problem aimed at finding the optimal serving cluster that satisfy the QoS requirements for each user and the corresponding power allocation vector.

Let $\mathcal{M} = \{\mathcal{M}_i, \forall i \in \mathcal{N}\}$ denote the variable for AP clustering. Let $\mathcal{P} = \{P_{T,ik}, \forall i \in \mathcal{N}, \forall k \in \mathcal{K}\}$ denote the transmit power variable for the multi-connectivity users. Based on this, we use a scalarization to formulate the general multi-objective optimization problem of APs clustering and power allocation as

$$\max_{\mathcal{P}, \mathcal{M}} \frac{1}{N} \sum_{i=1}^N \mathbb{1}(\mathcal{M}_i(t) = \mathcal{M}_i(t-1)) + \frac{\sum_{i=1}^N b_i}{nP_{\text{total}}/(1 - \varepsilon_{\max})} \quad (14a)$$

$$\text{s.t. } C_1 : \varepsilon_i \leq \varepsilon_{\max}, \quad \forall i \quad (14b)$$

$$C_2 : P_{T,ik} \leq P_{\max}, \quad \forall i, k, t \quad (14c)$$

$$C_3 : |\mathcal{M}_i(t)| \geq 1, \quad \forall i, t \quad (14d)$$

$$C_4 : \gamma_i^{\mathcal{M}_i}(t) \geq \gamma_{\text{th}}, \quad \forall i, t \quad (14e)$$

where ε_{\max} is the maximum error threshold tolerable for the reliable communication, b_i is the number of information bits transmitted to AU i , n is the block-length, and $P_{\text{total}} = \sum_{k=1}^K \sum_{i=1}^N P_{T,ik}$ is total transmitted power. The first term in (14a) aims to maintain the stability of the serving clusters for the AUs moving within the area, while the second term seeks to maximize the number of bits successfully transmitted using the minimum total transmit power. It can be observed that given ε_{\max} , n , and b_i are constant, maximizing the successfully transmitted bits is equivalent to minimizing the total power consumption from all APs.

D. Mobility Model

In this work, we employ a realistic and tractable mobility model to capture the mobility of UAVs. In particular, we use the model provided in [27] using coupled stochastic differential equations. By utilizing estimated positions instead of actual ones, the model incorporates more realistic device trajectories and considers imperfect navigation. The advantage of this approach lies in its ability to generate smoother and realistic trajectories. Additionally, it provides better control over velocity through correlation parameters, which influence stability and mobility based on distance-velocity relationships. Additional variance parameters scale Brownian perturbations, offering flexibility in introducing stochastic variations. For detailed explanations of the model, please refer to the original work [27].

E. User Handling

In a multi-connectivity wireless interference network, the dynamic clustering of APs depends on the number of users being served by the network. The arrival and departure of users within the network's coverage area influence the clustering decisions. Therefore, for a more realistic and dynamic scenario, our system needs to efficiently manage users entering and

leaving the coverage area without disrupting the already established clusters.

1) *Users Entering the Coverage Area:* When a completely new mobile user enters the coverage area of the system, they were not previously associated with the system. As a result, they become part of the active user group and are served by a new AP cluster. The formation of a new serving clusters without affecting the other clusters ensures that new users seamlessly receive services within the existing system framework.

2) *User Leaves the Coverage Area:* On the other hand, active users can become inactive, e.g., by moving out of the service area or switching off their device. As a result, they transition from an active to a non-active state and are no longer served by the AP cluster they were previously associated with. The freed APs can then be used to become part of the serving clusters of the active users. This allows to efficient management of resources and ensure optimal service distribution to active users.

IV. HMARDL FOR DYNAMIC CLUSTERING AND POWER ALLOCATION

In this section, we present a hierarchical learning framework to decompose the joint cluster reconfiguration and power allocation problem in (14a) by exploiting the dependency between them. In this framework, the edge cloud having global observations learns the optimal clustering policy, also referred as the high-level policy, for the connected APs serving the AUs within the edge cloud coverage area. While each AP acting as a single agent uses local observations to learn the optimal power allocation policy, also referred as the low-level policy, for the allocated AUs. Both the clustering and power allocation policies are governed by their respective observation spaces, action spaces and the reward functions.

A. Problem Decomposition

As shown in [1], the original problem remains scalable when the number of APs in the service area is limited. However, as the number of APs increases, the action space grows significantly, making it challenging to find a solution for the joint objective function within a finite time. To address this challenge, we decompose the optimization problem in (14a) into two subproblems, separating the tasks of cluster reconfiguration and power allocation.

1) *Subproblem 1: Optimal Cluster Reconfiguration:* The first subproblem aims to maintain the stability of the serving clusters, which is formulated as:

$$\Gamma : \max_{\mathcal{M}} \frac{1}{N} \sum_{i=1}^N \mathbb{1}(\mathcal{M}_i(t) = \mathcal{M}_i(t-1)) \quad (15a)$$

$$\text{s.t. } C_1 - C_4. \quad (15b)$$

The problem poses a combinatorial challenge and is difficult to solve due to the non-convex nature of its objective function. Typically, there is no computationally efficient or systematic method for achieving an optimal solution to this type of problem. However, it is well-suited for an iterative RL approach. To ensure this subproblem remains bounded and converges

in time, we modify the problem by incorporating constraint C_4 into the objective function. Further details are given in Section IV-C.

2) *Subproblem 2: Optimal Power Allocation:* Consider a given fixed clustering policy π , the optimal power allocation policy $\mathcal{P}_{i,k}^*$ can be obtained as a solution to the following optimization problem for every t :

$$\mathcal{P}_{i,k}^* : \max_{\mathcal{P}} \frac{\sum_{i=1}^N b_i}{nP_{\text{total}}/(1 - \varepsilon_{\text{max}})} \quad (16a)$$

$$\text{s.t. } C_1 - C_4 \quad (16b)$$

The objective in (16a) is to maximize the number of bits transmitted while satisfying reliability constraints, with the least possible total transmitted power. The optimal power allocation $\mathcal{P}_{i,k}^*$ minimizes the transmitted power in the link between user i and the serving AP cluster for all user-AP links at each time t . Thus, $\mathcal{P}_{i,k}^*$ provides the optimal power allocation for any given clustering Γ .

B. Hierarchical MAPPO Framework

The H-MAPPO framework addresses the mobility management problem for multi-connectivity users by employing a hierarchical decision making structure, as shown in Figure 1. In this framework, the edge cloud first determines the high-level action, specifically the clustering strategy Γ for each user $i \in \mathcal{N}$, utilizing the conventional proximal policy optimization (PPO) algorithm. Subsequently, each low-level AP $k \in \mathcal{K}$ updates its power allocation policy $P_{T,ik}$ for each assigned user using the multi-agent proximal policy optimization (MAPPO) algorithm. This update is based on the assigned users N_k , their locations, and channel conditions. The interactions among the low-level agents collectively determine the system state for the high-level agent, prompting the edge cloud to revise its clustering strategy in the subsequent decision epoch. This hierarchical design effectively reduces the search space for each agent and enhances learning efficiency. In the following, we define the high-level and low-level RL components for the edge cloud and the APs, respectively.

C. High-Level: Dynamic Cluster Reconfiguration

First, we discuss the high-level agent in detail, in particular its observation space, action space, and reward function.

1) *High-Level Observation Space:* The observation space of the high-level agent, located at the edge cloud, must include network-level information about the connected APs and AUs for optimal clustering. The high-level observation space includes the location information of the AUs $\mathbf{x}, \mathbf{y}, \mathbf{z} = \{x_i, y_i, z_i \ \forall i\}$, user load of the APs $\mathcal{N} = \{\mathcal{N}_k, \forall k\}$, the channel condition between connected APs and the AUs $\mathbf{h} = \{h_{i,k}, \forall i, k\}$, and the current clustering $\mathcal{M} = \{\mathcal{M}_{i,k}, \forall i, k\}$. Consequently, the observation space of the high-level agent is expressed as:

$$\bar{\mathcal{S}}_t \triangleq \{\mathbf{x}(t), \mathbf{y}(t), \mathbf{z}(t), \mathbf{l}(t), \mathbf{h}(t), \mathcal{M}(t-1)\} \quad (17)$$

2) *High-Level Action Space:* At each time step, the main role of the high-level agent is to take an action $\bar{a}_t \triangleq [\mathcal{M}_1, \mathcal{M}_2, \dots, \mathcal{M}_N]$ which gives the serving cluster \mathcal{M}_i for each AU $i \in \mathcal{N}$.

3) *High-Level Reward Function*: The reward function for the high-level agent guides its policy π_θ parameterized by θ by rewarding stability in cluster configurations, i.e., by minimizing the number of cluster reconfigurations, as described in (15a). To connect the high-level policy with the low-level actions of the APs, the reward is structured around two key objectives: maintaining stable serving clusters for the AUs and reducing the number of AUs experiencing SINR outages. Thus, the agent is rewarded when clusters remain stable, provided that users are not in outage. The instantaneous reward r that the agent receives for a given action in a particular state is defined as:

$$\bar{r} = \frac{\omega_1}{N} \sum_{i=1}^N \mathbf{1}(\mathcal{M}_i(t) = \mathcal{M}_i(t-1)) - \frac{\omega_2}{N} \sum_{i=1}^N \mathbf{1}(O_i > O^{th}), \quad (18)$$

where the non-negative weights ω_i , $i \in \{1, 2\}$, are used to balance between the individual objectives. The reward \bar{r} in (18) increases when the number of stable clusters or non-outage users increases. The O_i is obtained from (10) and depends on the SINR threshold.

D. Low-Level: Multi-Agent Optimal Power Allocation

Through the action \bar{a}_t of the learned policy π_θ , the edge cloud assigns a serving cluster \mathcal{M}_i for each AU $i \in \mathcal{N}$. Consequently, an AP $k \in \mathcal{K}$ is allocated a set of users $\mathcal{N}_k \subseteq \mathcal{N}$ to be served by this AP. The APs, using a multi-agent learned policy, optimize the power allocation for their assigned users. To facilitate this, we outline the basic RL components for the low-level multi-agents in the following.

1) *Low-Level Observation Space*: The low-level observation space s_t^k is designed to encompass both local information pertinent to the agent and shared data from the higher level $s_t^k = \{\bar{s}_t^k, \bar{a}_t^k\}$. Specifically, the observation space for the k -th agent includes the assigned users $\mathcal{N}_k \subseteq \mathcal{N}$, their location information $\mathbf{x}, \mathbf{y}, \mathbf{z} = \{x_j, y_j, z_j : j \in \mathcal{N}_k\}$, the line-of-sight (LoS) conditions for assigned users $LoS_{j,k}, j \in \mathcal{N}_k$, and a set detailing the assigned clusters from the higher level $\mathcal{M}_k = \{\mathcal{M}_j, \forall j \in \mathcal{N}_k\}$. Consequently, the observation space of the low-level k -th agent is expressed as:

$$S_t^k \triangleq \{\mathbf{x}(t), \mathbf{y}(t), \mathbf{z}(t), LoS_{j,k}, \mathcal{M}_k(t)\} \quad (19)$$

2) *Low-Level Action Space*: The low-level agents at APs operate independently, utilizing a learned policy. At each time epoch t , the higher-level agent performs clustering actions for each user within the service area, and each low-level agent k takes the action a_t^k , which determines the optimal power allocation $P_{j,k}^*, \forall j \in \mathcal{N}_k$. An agent k develops a policy π_{θ_k} parameterized by θ_k that exploits the dynamic characteristics of the channel and the clustering from the higher level to optimize power allocations from various APs in the cluster. The policy's primary objective is to maximize the objective function (16a) while adhering to constraints. The action space of low-level agent k is expressed as:

$$A_t^k \triangleq [P_{1,k}^*, P_{2,k}^*, \dots, P_{N_k,k}^*] \quad (20)$$

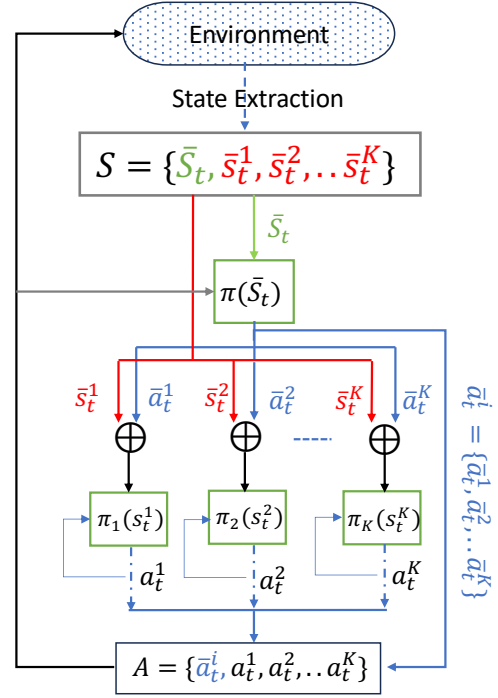


Figure 2. Proposed action-observation transition-driven H-MAPPO Framework.

3) *Low-Level Reward Function*: The reward for the low-level agent aims to increase the fraction of users associated to it, while using minimum power and satisfying the constraints. In particular, the instantaneous reward is expressed as a continuous function that seeks to minimize the total transmitted power while penalizing the violation of constraints. The low-level reward function r_t^k for agent k at time t is given as:

$$r_t^k = \left(1 - \omega_1 \frac{\sum_j^{N_k} P_{j,k}^*}{N_k P_{Tmax}}\right) - \frac{\omega_2}{N_k} \sum_{i=1}^{N_k} \mathbf{1}(\varepsilon_i > \varepsilon_{max}) \quad (21)$$

where the non-negative weights ω_i , $i \in \{1, 2\}$, are used to balance between the individual objectives. The reward r in (21) increases when the used transmit power is reduced, and decreases when the number of assigned users violating the DEP threshold ε_{max} increases. Towards this goal, we implement the MAPPO algorithm to derive the power allocation policy $P_{j,k}^*$.

E. The Proposed Hierarchical MAPPO Algorithm

An overview of the complete RL framework for the proposed H-MAPPO is presented in Figure 2. An algorithmic description of the proposed H-MAPPO framework is given in Algorithm 1. In the first episode, the high-level edge cloud agent selects the clustering of the APs. This clustering decision then updates the observation space for the low-level APs agents, allowing each AP to determine the power allocation based on the local observations, as detailed in lines 7 through 9 of Algorithm 1. After the edge cloud and APs perform their respective actions, the rewards are computed, and both the high-level and low-level policies are updated accordingly.

F. MAPPO Policy Training

In the MAPPO algorithm, each policy π_{θ_k} parameterized by θ_k , is a function that maps states to actions. The policy is typically represented by a neural network, which takes the state as input and outputs a probability distribution over the possible actions. Each policy is trained independently, meaning that the data collected from one policy is not used to train the other policies. However, the policies can share the same architecture and weights, and can be trained in parallel.

MAPPO uses the same core principles as single-agent PPO, with modifications to handle multiple agents and their interactions. Derived from the Trust Region Policy Optimization algorithm [36], [37], PPO introduces a clipped surrogate objective to enhance stability in policy updates. Each agent updates its policy to maximize the expected reward, using the following clipped surrogate objective [38]:

$$L_k^{\text{CLIP}}(\theta_k) = \mathbb{E}_t \left[\min \left\{ \rho_t(\theta_k) \hat{A}_t^k, \text{clip}(\rho_t(\theta_k), 1 - \eta, 1 + \eta) \hat{A}_t^k \right\} \right] \quad (22)$$

where $\rho_t(\theta_k)$ is the probability ratio between the new and old policies for the action a_t^k :

$$\rho_t(\theta_k) = \frac{\pi_{\theta_k}(a_t^k | s_t^k)}{\pi_{\theta_{\text{old}}}(a_t^k | s_t^k)} \quad (23)$$

and \hat{A}_t^k is the advantage function estimate for agent k . The clipping parameter η controls the extent of policy updates to ensure stability.

Advantage estimation quantifies how much better an action is compared to the expected value. MAPPO employs Generalized Advantage Estimation (GAE) to reduce variance and improve stability:

$$\hat{A}_t^k = \sum_{l=0}^{\infty} (\gamma \lambda)^l \delta_{t+l}^k, \quad (24)$$

where δ_t^k is the temporal difference error for agent k :

$$\delta_t^k = r_t^k + \gamma V(s_{t+1}^k) - V(s_t^k). \quad (25)$$

Here, γ is the discount factor, λ is the GAE parameter, and $V(s_k)$ is the state value function for agent k . In MAPPO, each agent learns its policy independently, optimizing its objective based on individual experiences:

$$\theta_k \leftarrow \theta_k + \alpha \nabla_{\theta_k} L_k^{\text{CLIP}}(\theta_k), \quad (26)$$

where α is the learning rate. Agents interact within the environment, which provides feedback in the form of rewards that guide the policy updates.

G. Deployment Scenario

We formulate our problem as an MDP within OpenAI's Gym environment. Our hierarchical multi-agent framework is implemented using Ray's RLlib library [39]. RLlib offers a scalable, flexible, and efficient solution for training RL models across multiple nodes and GPUs. By harnessing Ray's

Algorithm 1 H-MAPPO based Dynamic Clustering and Power Allocation

Input: $K, N, \varepsilon_{\max}, P_{\max}$, and γ_i^{th}

Output: Clustering strategy Γ , Optimal power allocation $P_{i,k}^*$

```

1: for each episode  $\leftarrow 1$  to end do
2:   Initialize: High level observation space  $\bar{S}_t$  and low-level
   observation space for each agent  $S_t^i$ 
3:   while not done do
4:     if first episode then
5:       Only high-level agent accepts observation space
       and returns the action space
6:     end if
7:      $\bar{A}_t = \{\bar{a}_t^1, \bar{a}_t^2, \dots, \bar{a}_t^K\}$ : Action space from trained
   high level agent
8:      $S_t^i = \{\bar{a}_t^i, x_i(t), l_i(t), LoS_i\}$ : Updated observation
   space of a low-level agent  $i$ 
9:      $A_t = \{a_t^1, a_t^2, \dots, a_t^K\}$ : Action space from trained
   low-level agents
10:    Calculate the error probability from (8) using
    $\{\bar{A}_t, A_t\}$ 
11:    Obtain the high level reward using (18) and low-level
   reward using (21)
12:    Update the status of the users
13:  end while
14: end for

```

Table II
HYPERPARAMETERS EMPLOYED FOR TUNING OUR MODEL

Parameters	Value
Learning rate	10^{-5}
Batch size	4000
Entropy coefficient	auto
Iterations	$2 \cdot 10^6$
Discount factor (γ)	0.99
GAE parameter (λ)	1.0
PPO Clip parameter (η)	0.3

distributed computing capabilities, RLlib parallelizes simulations, experience collection, and model updates, significantly accelerating training processes and enabling the handling of large-scale RL tasks.

Given the discrete-time nature of our problem, after each iteration, the higher-level agent's policy generates values for the cluster reconfiguration indicator, while the lower-level agents' policies generate the outage and transmit power indicators. Using these values, the high-level reward (18) and the low-level reward (21) for each agent are calculated and fed back to the respective agents.

The initial agent hyperparameters are summarized in Table II, having been empirically determined through multiple iterations. The source code of our implementation for reproducing all of the shown results will be made publicly available with the final version of the paper.

V. NUMERICAL EVALUATION

In this section, we showcase the effectiveness of our proposed H-MAPPO implementation for solving (14a). Additionally, we benchmark our H-MAPPO algorithm against the following baseline methods:

- **MSAC:** A centralized approach called masked soft actor-critic (MSAC) based clustering and power allocation from [1].
- **MAPPO:** A completely distributed approach without any hierarchical policy division based clustering and power allocation, where each agent decides to join the serving cluster for a user and allocated power.
- **Opportunistic:** An opportunistic clustering approach from [15], where a central entity opportunistically decide to include an O-RU (AP) in a cluster for user service based on channel gains.
- **Closest:** A simple approach in which only the nearest O-RU (AP) serves a user with maximum power.

For the numerical evaluation, there are $N = 6$ users in a square area of $3 \text{ km} \times 3 \text{ km}$. They are served by $K = 19$ APs, which are placed randomly within this area at a height of 25 m. Each AP is equipped with $L = 16$ antennas. The model of the path-loss follows [28], where we set the carrier frequency to 2.0 GHz to accommodate a broader range for command and control traffic for the UAVs. The noise power at the receiver is given as $\sigma^2 = N_0 B$, where $B = 10 \text{ MHz}$ is the communication bandwidth, and $N_0 = -174 \text{ dBm/Hz}$ is the noise spectral density. The UAVs move randomly following the mobility model described in Section III-D across the area. For a fair comparison, we keep all parameters of the communication system the same for all algorithms.

A. Learning Efficiency of H-MAPPO

We begin by evaluating the convergence and learning performance of the proposed action-observation transition-driven H-MAPPO algorithm, comparing it to the distributed MAPPO algorithm, which uses the conventional MAPPO method to the APs agents. In H-MAPPO, the clustering decision is centralized while power allocation is distributed, whereas in MAPPO, both clustering and power allocation decisions are distributed. As illustrated in Figure 3, agents utilizing the action-observation transition-driven H-MAPPO exhibit significantly faster convergence and higher overall reward accumulation than those relying on the distributed MAPPO approach. Specifically, the reward performance of the H-MAPPO algorithm experiences a steep rise in the early stages of training, stabilizing at a higher value in a shorter time compared to the slower and less consistent learning trajectory of MAPPO.

Although both algorithms show some fluctuations in reward values, the action-observation transition-driven H-MAPPO achieves an estimated 15% improvement in overall rewards. This enhanced performance can be attributed to the algorithm's distinct ability to decouple the tasks of clustering and power allocation between the various APs. By allowing the high-level edge cloud to control clustering decisions, each AP acts independently as a PPO agent, iteratively adjusting its

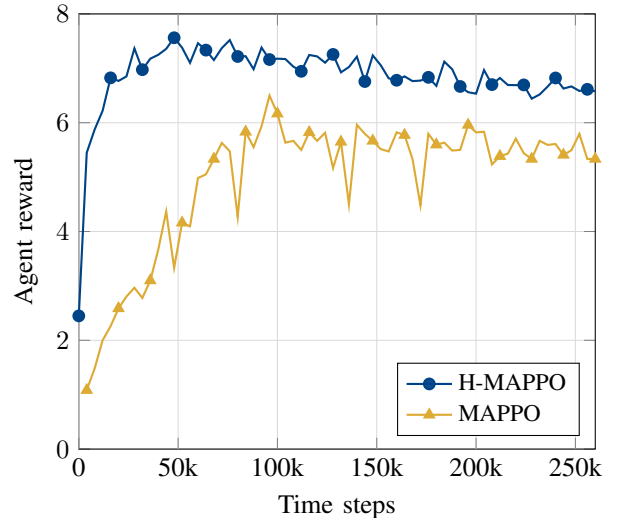


Figure 3. Numerical results comparing the rewards obtained during training iterations for both H-MAPPO and MAPPO.

power allocation strategy based on local observations of its environment. This hierarchical structure ensures that clustering and resource management decisions are more efficient and tailored to the specific conditions at each AP.

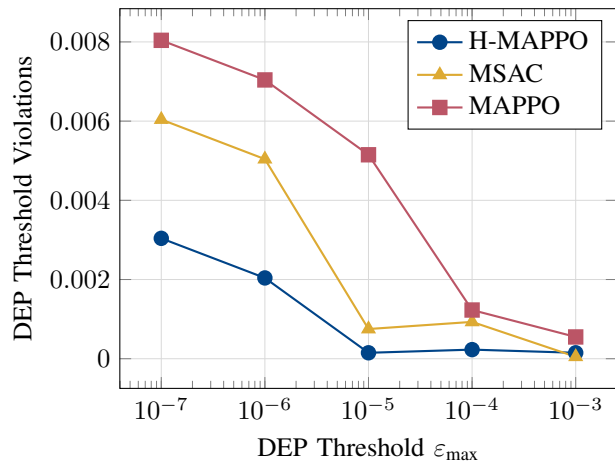
Moreover, the parallel training of all low-level APs agents further reduces training time and computational costs, as the system can learn more efficiently by distributing tasks across agents. The coordination between the high-level clustering decisions and the low-level power allocation adjustments enables the action-observation transition-driven H-MAPPO to optimize resource utilization and achieve superior performance. This hierarchical approach represents a notable improvement over the traditional MAPPO algorithm, where agents face greater difficulty balancing both clustering and power allocation simultaneously without a clear separation of responsibilities.

B. Reliability Performance

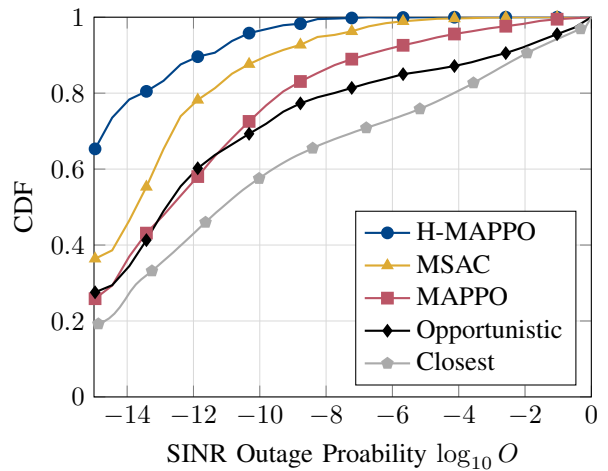
In Figure 4, we demonstrate the reliability performance of our proposed action-observation transition-driven H-MAPPO algorithm. One of the primary objectives of our problem is to ensure reliable data transmission with a DEP below a given threshold, i.e., $\varepsilon_i \leq \varepsilon_{\max}$.

The results for DEP threshold violations are presented in Figure 4(a) and the distribution of the SINR outage probability O in Figure 4(b). Although these two objectives are interdependent, in our proposed action-observation transition-driven H-MAPPO algorithm, the DEP threshold constraint governs the low-level policy, while the SINR outage constraint influences the high-level policy.

In Figure 4(a), we observe the results of the average DEP threshold violations experiences by the users under different schemes. It can be seen that the proposed H-MAPPO algorithm achieves comparable performance to the centralized MSAC for medium to high thresholds, whereas the fully distributed MAPPO suffers from a higher rate of outages. Since the Opportunistic and Closest schemes do not optimize for the reliability, the violations are very high



(a) DEP threshold violations experienced by the UAVs for different DEP thresholds ε_{\max} .



(b) CDF of the outage probability O experienced by the UAVs in service area.

Figure 4. Numerical results of the DEP threshold violation and the SINR outage probability O . (Section V-B)

compared to the learning-based algorithms (in the range of 0.890 to 0.989) and are therefore not shown in Figure 4(a).

Furthermore, as the DEP threshold decreases, the number of outages increases. This is expected, as maintaining a low error probability in a dynamic environment becomes challenging due to fluctuating channel conditions. However, for small thresholds ε_{\max} , our proposed H-MAPPO algorithm significantly outperforms the other schemes.

Next, in Figure 4(b), we present the SINR outage probability results. The CDF illustrates the distribution of outage probabilities O experienced by users as they move through the service area. As can be seen from the figure, the proposed H-MAPPO algorithm outperforms all comparison strategies. In particular, for the proposed H-MAPPO algorithm, the CDF is close to one when the outage probability is around 10^{-8} , i.e., the SINR outage probability experienced by a user almost never exceeds this value. For the centralized MSAC scheme, this value is closer to 10^{-5} , i.e., three orders of magnitude greater than for our proposed algorithm. However, both algorithms perform significantly better than the baselines MAPPO, Opportunistic, and Closest. The superior performance of H-MAPPO stems from its ability to adapt to strict reliability constraints through dynamic power control by low-level agents, guided by the maximum error threshold. By considering user positions, LoS conditions, and spatial relationships between neighboring APs, the algorithm minimizes interference and ensures reliability.

Although the Opportunistic strategy performs better than the Closest approach, the latter reduces interference by limiting the number of serving APs per user. However, this reduction in interference comes at the cost of reduced received power, which increases the likelihood of outages. Both strategies fall short of optimizing for the stricter reliability demands of the system. These results highlight the effectiveness of our hierarchical framework, which combines the reliability of a centralized approach with the scalability and efficiency of a distributed approach.

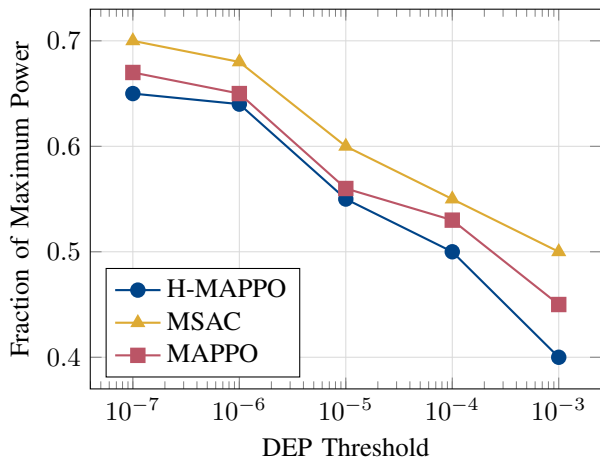
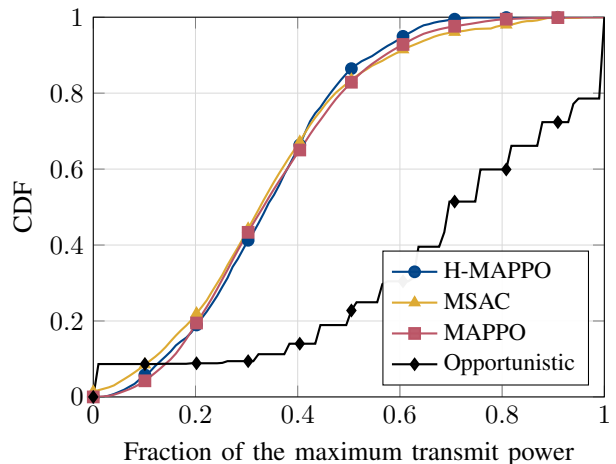
C. Transmit Power Performance

The second objective of our problem is to minimize the total transmitted power from the serving clusters while ensuring the system meets its reliability performance targets. Achieving this with minimal power is crucial for system energy efficiency. The comparison of the total transmitted power across different algorithms is shown in Figure 5. Since the transmit power in the Closest scheme is constant, it has been omitted from the graph.

As depicted in Figure 5(a), the proposed H-MAPPO algorithm achieves the DEP threshold with the lowest transmit power, followed by the fully distributed MAPPO. In contrast, the centralized MSAC requires the highest power. This is because MSAC, while consuming more power, provides better reliability compared to MAPPO, which experiences more outages, as shown in Figure 4. The proposed H-MAPPO outperforms both in terms of reliability and power efficiency. The high-level clustering policy in H-MAPPO allows the edge cloud to select the most favorable APs for the serving clusters, whereas the fully distributed approach may involve suboptimal APs, leading to more power consumption. Additionally, it is observed that as the DEP requirement becomes stricter, the total transmitted power increases to boost the SINR and reduce transmission errors.

The Closest scheme operates with a single AP at maximum power, resulting in a constant graph at $1/K$, i.e., $1/19 \approx 0.05$ for this particular example. Meanwhile, the Opportunistic scheme, which is not optimized for meeting reliability constraints, uses on an average over 90% of the available power and is unaffected by the DEP thresholds. Therefore, these schemes are not shown in Figure 5(a). However, the transmit power distribution for Opportunistic is presented alongside other schemes in Figure 5(b).

The observations from Figure 5(b) reveal that the learning-based cluster and power allocation schemes use less than 60% of the maximum available transmit power 90% of the time. While non-learning based algorithms use less than

(a) Fraction of total transmitted power for different DEP thresholds ϵ_{\max} .

(b) CDF of the total transmit power.

Figure 5. Numerical results of fraction of maximum power utilized and the distribution of the total transmit power of the system normalized by the maximum available power. (Section V-C)

60% of the maximum available transmit power only 30% of the time. This highlights that these learning-based methods not only excel at mitigating outages and meeting stringent reliability requirements, but they also achieve these goals with significantly reduced total transmitted power.

D. Clustering Size and Scalability Performance

The third objective in our problem is the formation of clusters. The distribution of the average cluster size for serving mobile UAVs is depicted in Figure 6. Notably, the distribution for H-MAPPO is centered around smaller cluster sizes, indicating that the high-level clustering decision typically involves half or fewer APs per serving cluster. Having a smaller number of APs serving a user simplifies the coordination and is therefore beneficial. Through training, the high-level agent in H-MAPPO effectively balances SINR outage requirements and the number of APs in each cluster. In particular, almost no clusters with more than 11 APs have been formed by the H-MAPPO algorithm. The cluster size distribution of the H-MAPPO reflects that the scheme uses less than half of the APs for forming clusters. While the distribution from MAPPO reflects that it uses more than 11 APs with similar probability. The H-MAPPO shows the highest probability for a cluster size of 7, whereas for MSAC and MAPPO, the peak occurs at 8. The variation in cluster sizes is due to the separation of clustering and power allocation in H-MAPPO, where power is optimized for a fixed cluster size. In contrast, while MSAC centralizes the power allocation and clustering decisions, directly influencing cluster sizes, MAPPO fully decentralizes these decisions, resulting in a wider distribution of cluster sizes.

Meanwhile, the Opportunistic scheme, driven by favorable channel conditions and full power transmission, often involves more than 50% of APs in clusters, leading to excessive power usage. The Closest algorithm uses only single AP for connectivity, its results are thus not shown in Figure 6. Additionally, it is noteworthy that both H-MAPPO and

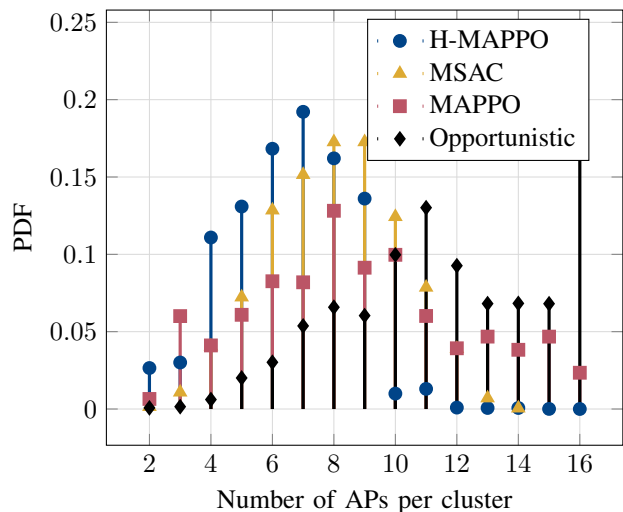


Figure 6. Numerical results of the average cluster size for serving mobile UAVs.

MSAC exhibit near-zero probability for cluster sizes greater than or equal to 13, whereas the Opportunistic scheme peaks at a cluster size of 16, essentially involving all APs in the cluster.

To underscore the need for the hierarchical approach over the centralized method for joint clustering and power allocation, we assess the scalability of our proposed H-MAPPO algorithm in comparison to the centralized MSAC approach. The results in Figure 7 show the time required to complete an episode in both H-MAPPO and MSAC, relative to the maximum episode time, as the number of APs in the network increases. The findings highlight the superior scalability of the H-MAPPO algorithm, where the decision-making for clustering and power allocation is distributed across two levels: the high-level edge cloud for clustering and the low-level APs for power control. In contrast, MSAC relies on a single centralized agent to manage all decisions, making it less scalable as the network grows.

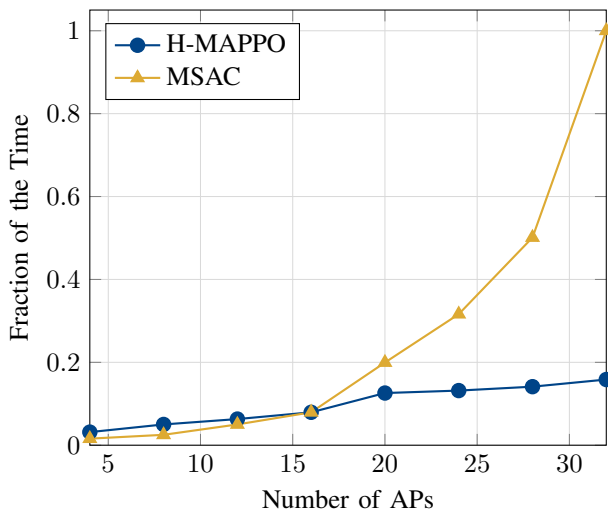


Figure 7. Numerical results of the relative time needed to complete an episode during policy training.

A key observation from the results is that when the number of APs doubles from 16 to 32, the training time for H-MAPPO increases by only about 10% per episode, while the same increase in MSAC leads to a 90% rise in training time. This stark difference underscores the efficiency of H-MAPPO, as it distributes the decision-making process across agents, reducing the computational load on a single entity. Moreover, this improvement in scalability does not come at the cost of performance. The distributed nature of H-MAPPO allows it to maintain or even improve system performance while scaling more efficiently than the centralized MSAC approach.

VI. CONCLUSION

In this paper, we have investigated the mobility management for multi-connectivity users in a wireless interference network under stringent reliability requirements. The mobility management problem involves joint dynamic cluster reconfiguration and energy-efficient power allocation with stringent QoS requirements. To solve it, we first divided the joint problem into two subproblems and propose a hierarchical two-layer H-MAPPO-based mobility management scheme. For the first layer of H-MAPPO, we have transformed the original multi-connectivity subproblem into a cluster reconfiguration updating problem, and leveraged the single agent PPO algorithm to output an optimized clustering action. For the second layer, each AP acts as an independent agent responsible for efficient power allocation to their assigned users using the MAPPO algorithm. The learning efficiency is improved through a novel action-observation transition mechanism that makes the convergence of the two layers possible.

Extensive simulation results verify the effectiveness of the proposed H-MAPPO scheme in reducing both outage probability and total transmit power. H-MAPPO achieves an outage probability near 10^{-6} and operates below 60% of maximum transmit power in 90% of instances, compared to only 30% for opportunistic clustering methods. These results underscore its advantage in enhancing reliability and power efficiency for serving mobile UAVs.

In this work, we focused on user mobility within a single cloud's service area, with a single agent responsible for intra-cloud cluster reconfiguration. A natural extension of this work involves investigating scenarios where user mobility spans multiple clouds, necessitating inter-cloud cluster reconfiguration involving multiple agents.

REFERENCES

- [1] I. A. Meer, K.-L. Besser, M. Ozger, D. Schupke, H. V. Poor, and C. Cavdar, "Learning based dynamic cluster reconfiguration for UAV mobility management with 3D beamforming," in *Proceedings of the 2024 IEEE International Conference on Machine Learning for Communication and Networking (ICMLCN)*, IEEE, May 2024, pp. 486–491. DOI: [10.1109/ICMLCN59089.2024.10625071](https://doi.org/10.1109/ICMLCN59089.2024.10625071).
- [2] S. Bassoy, H. Farooq, M. A. Imran, and A. Imran, "Coordinated multi-point clustering schemes: A survey," *IEEE Communications Surveys & Tutorials*, vol. 19, no. 2, pp. 743–764, 2017. DOI: [10.1109/COMST.2017.2662212](https://doi.org/10.1109/COMST.2017.2662212).
- [3] F. Hu, Y. Deng, and A. H. Aghvami, "Scalable multi-agent reinforcement learning for dynamic coordinated multipoint clustering," *IEEE Transactions on Communications*, vol. 71, no. 1, pp. 101–114, Jan. 2023. DOI: [10.1109/TCOMM.2022.3220870](https://doi.org/10.1109/TCOMM.2022.3220870).
- [4] W. Mei, Q. Wu, and R. Zhang, "Cellular-connected UAV: Uplink association, power control and interference coordination," *IEEE Transactions on Wireless Communications*, vol. 18, no. 11, pp. 5380–5393, Nov. 2019. DOI: [10.1109/TWC.2019.2936021](https://doi.org/10.1109/TWC.2019.2936021).
- [5] A. Checko, H. L. Christiansen, Y. Yan, *et al.*, "Cloud RAN for mobile networks—a technology overview," *IEEE Communications Surveys & Tutorials*, vol. 17, no. 1, pp. 405–426, 2015. DOI: [10.1109/COMST.2014.2355255](https://doi.org/10.1109/COMST.2014.2355255).
- [6] E. Björnson and L. Sanguinetti, "Making cell-free massive MIMO competitive with MMSE processing and centralized implementation," *IEEE Transactions on Wireless Communications*, pp. 77–90, Jan. 2020. DOI: [10.1109/TWC.2019.2941478](https://doi.org/10.1109/TWC.2019.2941478).
- [7] B. Matthiesen, A. Zappone, K.-L. Besser, E. A. Jorswieck, and M. Debbah, "A globally optimal energy-efficient power control framework and its efficient implementation in wireless interference networks," *IEEE Transactions on Signal Processing*, vol. 68, pp. 3887–3902, 2020. DOI: [10.1109/TSP.2020.3000328](https://doi.org/10.1109/TSP.2020.3000328).
- [8] Y. Dai, J. Liu, M. Sheng, N. Cheng, and X. Shen, "Joint optimization of BS clustering and power control for NOMA-enabled CoMP transmission in dense cellular networks," *IEEE Transactions on Vehicular Technology*, vol. 70, no. 2, pp. 1924–1937, Feb. 2021. DOI: [10.1109/TVT.2021.3055769](https://doi.org/10.1109/TVT.2021.3055769).
- [9] M. Simsek, T. Hobler, E. Jorswieck, H. Klessig, and G. Fettweis, "Multiconnectivity in multicellular, multiuser systems: A matching-based approach," *Proceedings of the IEEE*, vol. 107, no. 2, pp. 394–413, Feb. 2019. DOI: [10.1109/JPROC.2018.2887265](https://doi.org/10.1109/JPROC.2018.2887265).
- [10] K. Yu, Q. Yu, Z. Tang, *et al.*, "Fully-decoupled radio access networks: A flexible downlink multi-connectivity and dynamic resource cooperation framework," *IEEE Transactions on Wireless Communications*, vol. 22, no. 6, pp. 4202–4214, Jun. 2023. DOI: [10.1109/TWC.2022.3224010](https://doi.org/10.1109/TWC.2022.3224010).
- [11] C. Wei, K. Xu, X. Xia, *et al.*, "User-centric access point selection in cell-free massive MIMO systems: A game-theoretic approach," *IEEE Communications Letters*, vol. 26, no. 9, pp. 2225–2229, Sep. 2022. DOI: [10.1109/LCOMM.2022.3186350](https://doi.org/10.1109/LCOMM.2022.3186350).
- [12] Z. Liu, J. Zhang, Z. Liu, D. W. K. Ng, and B. Ai, "Joint cooperative clustering and power control for energy-efficient cell-free XL-MIMO with multi-agent reinforcement learning," *IEEE Transactions on Communications*, 2024. DOI: [10.1109/TCOMM.2024.3415596](https://doi.org/10.1109/TCOMM.2024.3415596), Early Access.

- [13] B. Banerjee, R. C. Elliott, W. A. Krzymieñ, and M. Medra, "Access point clustering in cell-free massive MIMO using conventional and federated multi-agent reinforcement learning," *IEEE Transactions on Machine Learning in Communications and Networking*, vol. 1, pp. 107–123, 2023. DOI: 10.1109/TMLCN.2023.3283228.
- [14] T. T. Nguyen, N. D. Nguyen, and S. Nahavandi, "Deep reinforcement learning for multiagent systems: A review of challenges, solutions, and applications," *IEEE Transactions on Cybernetics*, vol. 50, no. 9, pp. 3826–3839, Sep. 2020. DOI: 10.1109/TCYB.2020.2977374.
- [15] R. Beerten, V. Ranjbar, A. P. Guevara, and S. Pollin, *Cell-free massive MIMO in the O-RAN architecture: Cluster and handover strategies*, Jan. 2023. arXiv: 2301.07618v1 [eess.SP].
- [16] I. A. Meer, M. Ozger, D. A. Schupke, and C. Cavdar, "Mobility management for cellular-connected UAVs: Model-based versus learning-based approaches for service availability," *IEEE Transactions on Network and Service Management*, vol. 21, no. 2, pp. 2125–2139, Apr. 2024. DOI: 10.1109/TNSM.2024.3353677.
- [17] B. Galkin, E. Fonseca, R. Amer, L. A. DaSilva, and I. Dusparic, "REQIBA: Regression and deep Q-learning for intelligent UAV cellular user to base station association," *IEEE Transactions on Vehicular Technology*, vol. 71, no. 1, pp. 5–20, Jan. 2022. DOI: 10.1109/TVT.2021.3126536.
- [18] Y. Chen, X. Lin, T. Khan, and M. Mozaffari, "Efficient drone mobility support using reinforcement learning," in *Proceedings of the 2020 IEEE Wireless Communications and Networking Conference (WCNC)*, IEEE, May 2020. DOI: 10.1109/WCNC45663.2020.9120595.
- [19] A. Azari, F. Ghavimi, M. Ozger, R. Jantti, and C. Cavdar, "Machine learning assisted handover and resource management for cellular connected drones," in *Proceedings of the 2020 IEEE 91st Vehicular Technology Conference (VTC2020-Spring)*, IEEE, May 2020. DOI: 10.1109/VTC2020-Spring48590.2020.9129453.
- [20] Y. Deng, I. A. Meer, S. Zhang, M. Ozger, and C. Cavdar, "D3QN-based trajectory and handover management for UAVs co-existing with terrestrial users," in *Proceedings of the 21st International Symposium on Modeling and Optimization in Mobile, Ad Hoc, and Wireless Networks (WiOpt)*, IEEE, Aug. 2023, pp. 103–110. DOI: 10.23919/WiOpt58741.2023.10349832.
- [21] Y. Al-Eryani, M. Akrouf, and E. Hossain, "Multiple access in cell-free networks: Outage performance, dynamic clustering, and deep reinforcement learning-based design," *IEEE Journal on Selected Areas in Communications*, vol. 39, no. 4, pp. 1028–1042, Apr. 2021. DOI: 10.1109/JSAC.2020.3018825.
- [22] I. A. Meer, K.-L. Besser, M. Ozger, H. V. Poor, and C. Cavdar, "Reinforcement learning based dynamic power control for UAV mobility management," in *Proceedings of the 57th Asilomar Conference on Signals, Systems, and Computers*, IEEE, Oct. 2023, pp. 724–728. DOI: 10.1109/IEEECONF59524.2023.10477032.
- [23] W. Shi, J. Li, H. Wu, C. Zhou, N. Cheng, and X. Shen, "Drone-cell trajectory planning and resource allocation for highly mobile networks: A hierarchical DRL approach," *IEEE Internet of Things Journal*, vol. 8, no. 12, pp. 9800–9813, Jun. 2021. DOI: 10.1109/JIOT.2020.3020067.
- [24] A. Alwarafy, B. S. Ciftler, M. Abdallah, M. Hamdi, and N. Al-Dhahir, "Hierarchical multi-agent DRL-based framework for joint multi-RAT assignment and dynamic resource allocation in next-generation hetnets," *IEEE Transactions on Network Science and Engineering*, vol. 9, no. 4, pp. 2481–2494, Jul. 2022. DOI: 10.1109/TNSE.2022.3164648.
- [25] T. Zhang, J. Xue, Y. Xu, *et al.*, "Handover-free multi-connectivity mobility management for downlink FD-RAN: A hierarchical DRL based approach," *IEEE Transactions on Cognitive Communications and Networking*, 2024. DOI: 10.1109/TCCN.2024.3452639, Early Access.
- [26] Ö. T. Demir, M. Masoudi, E. Björnson, and C. Cavdar, "Cell-free massive MIMO in O-RAN: Energy-aware joint orchestration of cloud, fronthaul, and radio resources," *IEEE Journal on Selected Areas in Communications*, vol. 42, no. 2, pp. 356–372, Feb. 2024. DOI: 10.1109/jsac.2023.3336187.
- [27] P. J. Smith, I. Singh, P. A. Dmochowski, J. P. Coon, and R. Green, "Flexible mobility models using stochastic differential equations," *IEEE Transactions on Vehicular Technology*, vol. 71, no. 4, pp. 4312–4321, Apr. 2022. DOI: 10.1109/TVT.2022.3146407.
- [28] *Enhanced LTE support for aerial vehicles*, 3GPP TR 36.777, version 15.0.0, 3GPP, Dec. 2017.
- [29] A. Colpaert, E. Vinogradov, and S. Pollin, "3D beamforming and handover analysis for UAV networks," in *Proceedings of the 2020 IEEE Globecom Workshops (GC Wkshps)*, IEEE, Dec. 2020. DOI: 10.1109/GCWkshps50303.2020.9367570.
- [30] A. Lancho, G. Durisi, and L. Sanguinetti, "Cell-free massive MIMO for URLLC: A finite-blocklength analysis," *IEEE Transactions on Wireless Communications*, vol. 22, no. 12, pp. 8723–8735, Dec. 2023. DOI: 10.1109/TWC.2023.3265303.
- [31] H. Ren, C. Pan, Y. Deng, M. Elkashlan, and A. Nallanathan, "Joint pilot and payload power allocation for massive-MIMO-enabled URLLC IIoT networks," *IEEE Journal on Selected Areas in Communications*, vol. 38, no. 5, pp. 816–830, May 2020. DOI: 10.1109/JSAC.2020.2980910.
- [32] A. A. Nasir, H. D. Tuan, H. Q. Ngo, T. Q. Duong, and H. V. Poor, "Cell-free massive MIMO in the short blocklength regime for URLLC," *IEEE Transactions on Wireless Communications*, vol. 20, no. 9, pp. 5861–5871, Sep. 2021. DOI: 10.1109/TWC.2021.3070836.
- [33] Y. Polyanskiy, H. V. Poor, and S. Verdú, "Channel coding rate in the finite blocklength regime," *IEEE Transactions on Information Theory*, vol. 56, no. 5, pp. 2307–2359, May 2010. DOI: 10.1109/TIT.2010.2043769.
- [34] R. Devassy, G. Durisi, P. Popovski, and E. G. Strom, "Finite-blocklength analysis of the ARQ-protocol throughput over the Gaussian collision channel," in *Proceedings of the 2014 6th International Symposium on Communications, Control and Signal Processing (ISCCSP)*, IEEE, May 2014, pp. 172–177. DOI: 10.1109/ISCCSP.2014.6877843.
- [35] S. Amari and R. Misra, "Closed-form expressions for distribution of sum of exponential random variables," *IEEE Transactions on Reliability*, vol. 46, no. 4, pp. 519–522, Dec. 1997. DOI: 10.1109/24.693785.
- [36] S. Roostaie and M. M. Ebadzadeh, *EnTRPO: Trust region policy optimization method with entropy regularization*, Oct. 2021. arXiv: 2110.13373 [cs.LG].
- [37] N. Peng, Y. Lin, Y. Zhang, and J. Li, "AoI-aware joint spectrum and power allocation for internet of vehicles: A trust region policy optimization-based approach," *IEEE Internet of Things Journal*, vol. 9, no. 20, pp. 19916–19927, Oct. 2022. DOI: 10.1109/JIOT.2022.3172472.
- [38] J. Schulman, F. Wolski, P. Dhariwal, A. Radford, and O. Klimov, *Proximal policy optimization algorithms*, Aug. 2017. arXiv: 1707.06347 [cs.LG].
- [39] E. Liang, R. Liaw, P. Moritz, *et al.*, *RLlib: Abstractions for distributed reinforcement learning*, Jun. 2018. arXiv: 1712.09381v4 [cs.AI].